Laser Plasma Production of Metal and Metal Compound Complexes with Polycyclic Aromatic Hydrocarbons†

T. M. Ayers, B. C. Westlake, and M. A. Duncan*

Department of Chemistry, University of Georgia, Athens, Georgia 30602-2556

Received: May 4, 2004; In Final Form: June 17, 2004

Gas-phase complexes of metals and/or metal compounds with polycyclic aromatic hydrocarbons (PAHs) are produced by covaporization of materials in a laser plasma source and detected using a time-of-flight mass spectrometer. Mixtures of metal powder, metal salts, metal oxides, or other materials with the PAH of interest are ablated and ionized with a pulsed Nd:YAG laser. Mass spectroscopy reveals that transition and rare earth metals efficiently produce both monoligand and sandwich complexes of the form $M^+(PAH)_x$, with $x = 1, 2$. Surprisingly, both iron and cobalt resist the formation of complexes when pure metal powder is employed, but produce them efficiently when salts, oxides, or organometallics are employed. Covaporization of the organometallic-π complexes iron cyclopentadienyl and dibenzene chromium with PAHs yields both homoligand and heteroligand complexes. Transition metal oxides and chlorides produce monoligand complexes exclusively. In contrast, rare earth oxides produce both monoligand and sandwich complexes, presumably due to the increased ionic radius of the metal center.

Introduction

New techniques employing lasers and molecular beams have made it possible to produce a fascinating variety of metal−aromatic sandwich complexes and organometallic cluster materials. Molecular beam experiments performed by Kaya and co-workers successfully produced transition metal multidecker sandwich complexes with benzene,[1−3] ferrocene,[4] and C_{60}.[5,6] In addition, Kaya and co-workers have produced sandwich complexes of metals with cyclooctatetraene (COT).[7] Other metal−fullerene complexes have been produced and studied by Martin and co-workers,[8−11] by Kaya and co-workers,[12−15] and by our research group.[16,17] Martin and co-workers were able to produce multiatom coatings of transition metals on C_{60} or C_{70} using an inert gas condensation source employing laser vaporization and a fullerene oven.[8−11] In work related to the fullerene studies, metal complexes with polycyclic aromatic hydrocarbons (PAHs) have been produced by Dunbar and co-workers,[18,19] by our group,[20−24] and by others.[25−27] We have shown that these species produce both sandwich and multiple-decker sandwich complexes, as well as adducts with multiple metal atoms attached to PAH molecules. The present work investigates new strategies for the formation of metal−PAH complexes, as well as trends in the tendencies of metals and metal compounds to form these systems.

PAHs occur in many natural environments where carbon is present. They are produced in hydrocarbon combustion, and have been implicated as components of dust in the interstellar medium (ISM). The optical properties of PAHs are well-known; absorption, fluorescence, and phosphorescence of gas-phase molecules and thin films have been studied extensively.[28−31] Additionally, ionized PAHs have been suggested as carriers of the optical diffuse interstellar bands (DIBs)[32−36] and the unidentified infrared bands (UIBs).[37,38]

Metal−PAH complexes are particularly interesting due to their potential importance as new materials for organic conductors, as models for surface science and catalysis, and also as possible constituents of interstellar gas clouds. Theoretical models of intercalated graphite and carbon nanotubes often use PAHs to represent a finite section of the carbon surface.[39−42] Specifically, coronene ($C_{24}H_{12}$) is the smallest PAH molecule that possesses the essential structural elements of graphite. Some of the most important catalytic processes involve metal atoms or clusters attached to supports. Metal atoms and/or clusters bonded to the surface of a PAH molecule can provide models of such supported catalysts. Residual metal from the catalysts employed for carbon nanotube synthesis affect the binding of nanotubes in bundles, and metal binding to nanotube walls will be necessary to make wire connections in carbon nanotube circuits. Metal−PAH complexes also provide convenient models for these processes. In astrophysics, Serra and co-workers first suggested that iron−PAH complexes may exist in the interstellar medium (ISM).[43,44] Metal−PAH complexes have been implicated in the depletion of atomic metal and silicon in the ISM and as possible contributors to the DIBs and UIBs.[25,26,45]

The growing interest in metal−PAH systems has motivated several groups to produce these species in laboratory experiments. In 1994, Dunbar and co-workers were the first to observe metal−PAH ion complexes in gas-phase experiments using FT-ICR mass spectrometry.[18,19] From these experiments, they determined the binding kinetics of a variety of metal and nonmetal cations with PAHs. Our group used a laser vaporization cluster source and PAH film coated metal samples to produce multiple metal and sandwich complexes in molecular beams.[20−24] Competitive binding and photodissociation studies were successful in determining structural information and relative bonding strengths of metals with benzene, C_{60}, and coronene.[24] More recently, Bohme and co-workers produced the first reactivity study of a variety of ligands with the iron−coronene complex using a selected ion flow tube apparatus.[26] Theoretical studies to investigate metal binding sites and bond energies on PAHs have been conducted by Dunbar,[46] Klippenstein and co-workers,[47] and Jena and co-workers.[48] Klippenstein

† Part of the special issue "Tomas Baer Festschrift".

* Corresponding author. E-mail: maduncan@uga.edu.

10.1021/jp0480753 CCC: $27.50
Published on Web 08/13/2004

and co-workers suggested that the metal ion−coronene bond strength is comparable to its metal−benzene counterpart,[47] consistent with our experimental estimates.[24]

Though some progress has been made in the study of metal−PAH systems, the structures, bonding energetics, and reactivities of such complexes remain largely unexplored. Therefore, a more general method of producing these clusters would facilitate studies of their properties. It is conceivable that new metal−PAH species will be stable enough for isolation in bulk quantities, opening up new areas of organometallic chemistry. Here we investigate new strategies for the production of metal−PAH complexes. As shown below, laser ablation of samples combining PAH materials with a variety of pure metal, metal compound, or organometallic powders makes it possible to produce a remarkable variety of monoligand complexes and sandwiches. Trends in complex growth reveal insight into metal−PAH bonding energetics and the reactivity of metals at graphitic surfaces.

Experimental Section

The laser desorption time-of-flight mass spectrometer used in these experiments has been described previously.[49] It has the capability for high acceleration fields (up to 30 kV) and delayed-pulsed ion extraction for improved resolution.[50] A 4.8 mm stainless steel probe hollowed out to 2 mm depth is employed for the mounting of solid samples of various metal powders or metal salts with the chosen PAHs. The powders are mixed using a mortar and pestle and then packed firmly inside the hollow probe tip. Another variation of this experiment uses a stainless steel or aluminum flat-tipped probe, where the samples are mixed into a slurry with methanol (HPLC grade), applied with a pipet, and allowed to dry in air. Smooth sample surfaces are essential to obtain the best results in these laser desorption experiments. Once prepared, the samples are inserted into the mass spectrometer for analysis.

The metal powders used in this experiment consist of the first-row transition metals from titanium to copper and zirconium carbide of varying grain sizes (Aldrich, Alfa Aesar). No care is taken to prevent these metals from oxidizing since it is also of interest to study metal oxide complexes with PAHs. Various transition metal chloride salts are also studied for comparison with metal powders. Neodymium and uranium are used as representatives of the lanthanide and actinide series; the neodymium sample consisted of filings from a partially oxidized solid rod, whereas the source of uranium was the salt uranyl acetate (UAc). Organometallics tested include ferrocene, iron cyclopentadienyl benzene [Fe(cp)(bz)], and dibenzene chromium [$Cr(bz)_2$]. Aluminum was introduced inadvertently via the probe tips, and both sodium and potassium are present as impurities resulting from the handling of samples. Coronene (cor), $C_{24}H_{12}$, and pyrene (py), $C_{16}H_{10}$, are the PAHs of choice for these experiments. Their low vapor pressures allow the samples to reside in a vacuum for an indefinite period of time without being pumped away. All chemicals are used as received without further purification.

Desorption and ionization is accomplished by focusing (20 cm lens) the output of an Nd:YAG laser (Continuum Minilite) operating at either 532 or 355 nm onto the sample in the probe tip inside the mass spectrometer. The fluence of the laser is adjusted with a variable attenuator prior to focusing to optimize production of the desired complexes, so that energies less than 1 mJ/pulse are employed for most of these experiments. Once the material is vaporized, cations are accelerated down the flight tube at an energy of 10 keV and focused with an einzel lens before reaching the detector. Mass spectra are collected and averaged with a digital oscilloscope (LeCroy LT 341) and transferred to a PC via an IEEE-488 interface for processing.

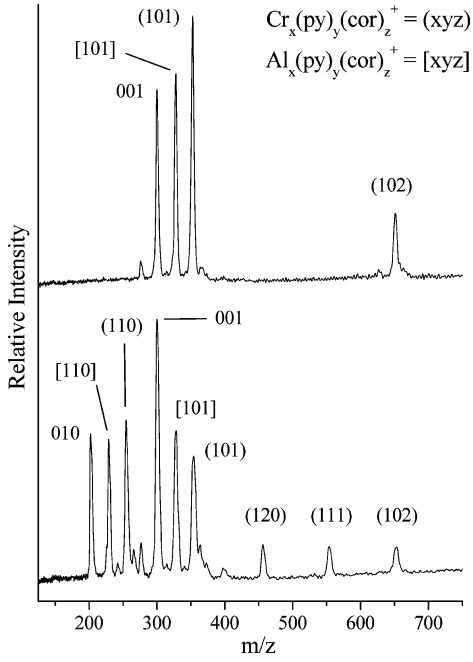

Figure 1. Mass spectra resulting from covaporization of chromium and coronene on an aluminum probe (upper trace) and chromium with a mixture of coronene and pyrene on an aluminum probe (lower trace). Complexes of the form $Cr_x(py)_y(cor)_z^+$ are indicated as (*xyz*), while similar complexes with aluminum are indicated as [*xyz*].

Results and Discussion

Transition Metal Powders + PAH. To explore a potentially facile method for the production of metal−PAH complexes, we investigated covaporization of samples composed of pure metal powder mixed with PAH powder. These experiments were carried out on all of the first-row transition metals with coronene, and selected experiments were also done with pyrene. Figure 1 shows a representative mass spectrum obtained from the vaporization (532 nm) of chromium/coronene powder (upper trace) and chromium powder mixed with both pyrene and coronene (1:1 molar). Several atomic ions are present in the low mass range of these spectra (not shown), including sodium, potassium, aluminum, and chromium (sodium and potassium are common impurities in many laser desorption experiments). The aluminum comes from the sample probe tip used in this experiment. No sodium− or potassium−PAH complexes were observed, but aluminum−PAH complexes are formed in addition to the desired chromium complexes. In both spectra, chromium−PAH monoligand and diligand complexes are present in large abundance. The diligand complexes here are presumed to be sandwiches because only small amounts of PAH dimers are observed without metal. Very little fragmentation of the PAH species is observed, probably because of the low laser power (0.5−1.0 mJ/pulse) used for these experiments. The only coronene fragment detected in this spectrum corresponds to the loss of one C_2 unit. This fragment ion is observed in nearly all experiments. The small intensity peak assigned as $Cr^+(cor)_2 - C_2$ could conceivably be assigned to an Al^+-(coronene)$_2$ complex, because this has the same mass. However, this peak is also observed in other experiments using different sample probes when no aluminum is present. It is therefore assigned to the chromium sandwich fragment ion. Results

similar to these chromium data are obtained for other transition metals, except that the efficiency of complex formation varies with the metal, as discussed below. We tried experiments using either the 532 or 355 nm output of the YAG laser for vaporization, but obtained usable signals only with the 532 nm wavelength. This was not an issue of laser power, because a wide variety of pulse energies were explored for both 532 and 355 nm. The 532 nm excitation worked best at lower laser pulse energy (0.5−1.0 mJ/pulse), and 355 nm excitation did not produce comparable results at any pulse energy level. At higher pulse energies, metal ions were detected, but complexes did not form efficiently, presumably because the plasma conditions were too hot.

Chromium shows no preference for forming coronene versus pyrene complexes, as the relative ion abundances are virtually equivalent for the Cr^+(py) and Cr^+(cor) ions. The same holds true for both chromium coronene and pyrene homoligand sandwich complexes and the Cr^+(py)(cor) mixed-ligand sandwich. Unlike our previous molecular beam experiments on chromium−coronene complexes,[22] we observe no multiple-metal complexes here with either coronene or pyrene and no complexes with more than two PAH molecules. In the molecular beam experiments, we employed a metal rod sample that was coated with a sublimed film of coronene. This film-coated rod sample was mounted in a normal laser vaporization cluster source with a pulsed nozzle expansion gas, and complexes were allowed to grow in a channel extending beyond the vaporization position. The present configuration has no expansion gas and no growth channel. The only opportunity for metal−PAH collisions is in the plume from the vaporization, where conditions are substantially hotter than room temperature. It is therefore understandable that smaller complexes, on average, result from the present conditions. Because of these conditions, we expect that any complexes that do form must have substantial bond energies. The complexes produced here are similar to those reported by Dunbar in FT-ICR experiments, where metal ions produced by laser vaporization were reacted with PAH vapor.[18,19]

In the spectrum shown in Figure 1, aluminum−PAH monoligand complexes are observed to form in amounts comparable to the chromium−PAH complexes. However, while good intensities are observed for diligand (sandwich) complexes of chromium, no such sandwich complexes are observed for aluminum. Dunbar and co-workers also reported that Al−coronene and Mg−coronene ions did not form sandwiches in their FT-ICR experiments.[18,19] This surprising observation can be understood by consideration of the binding tendencies seen before for many other ion−molecule complexes of aluminum and magnesium. The unusual clustering behavior of these cations was first investigated in theoretical studies by Bauschlicher and co-workers.[51−54] Their calculations suggested that diligand complexes for these ions with small molecules such as water or carbon dioxide would be bent instead of linear. This trend arises because the 3s electrons on Al^+ and Mg^+ are highly polarizable. The binding of an initial ligand induces a charge polarization, pushing electron density toward the opposite side of the metal ion. Additional ligands are repelled by this backside negative region, and tend to bind more on the same side of the cation as the first. Recent infrared photodissociation experiments performed by our group on $M^+(CO_2)_n$, M = Al or Mg, complexes found vibrational spectra consistent with those predicted for such bent structures.[55,56] Infrared spectra revealed that the $M^+(CO_2)_2$ complex is bent (C_{2v}) and the $M^+(CO_2)_3$ complex has a trigonal pyramid structure. Likewise, Nishi and co-workers recently observed similar bent structures for Mg^+-$(H_2O)_n$ complexes.[57] Following this same kind of logic, the binding of a PAH π cloud to Mg^+ or Al^+ should polarize these cations in the same way. If this polarization occurs, then a negative charge region would form on the metal ion on the side opposite the first PAH. In the PAH systems, however, the steric hindrance prevents binding of a second ligand on the same side of the cation as the first. The negative charge repels the second PAH, and therefore diligand complexes cannot form efficiently.

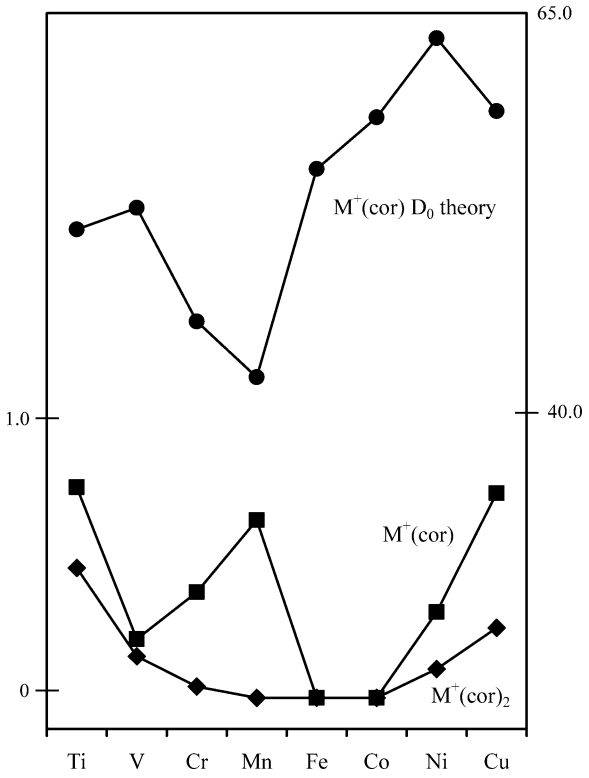

Figure 2. Graph displaying the relative abundances of the M^+(cor) and $M^+(cor)_2$ complexes normalized to the abundance of metal ion, and the comparison to the calculated M^+−coronene bond energies.[47] The left vertical axis indicates the relative tendency to form complexes, while the right vertical axis indicates the calculated bond energy (kcal/mol).

Figure 2 shows a graph summarizing the tendency for different transition metal ions to form monoligand and diligand complexes with coronene in these studies. A similar plot would be obtained for the selected metal−pyrene complexes studied. In all of these experiments, the intensity of the PAH cation mass peak is 2−3 times greater than that of any of the metal containing ion peaks. We can therefore assume that PAH concentration is not a limiting factor in these studies. However, metal ion concentration may vary from one system to another because of the different laser ablation efficiencies for different metals and their yield for ions as opposed to neutrals. The relative amounts of the complex ions are therefore normalized to the intensities of the respective atomic ion mass peaks for each metal. After this scaling, the relative amounts of the complexes shown in the figure can be associated approximately with the tendency for each metal ion to form complexes. For both the early transition metals, titanium through chromium, and the late transition metals, nickel and cobalt, both monoligand complexes and sandwiches were produced with good abundance. Manganese produced an abundance of the monoligand complex, but no sandwich was observed for this metal. Also, to our surprise, no iron or cobalt complexes with coronene were observed by this method, even though large amounts of the

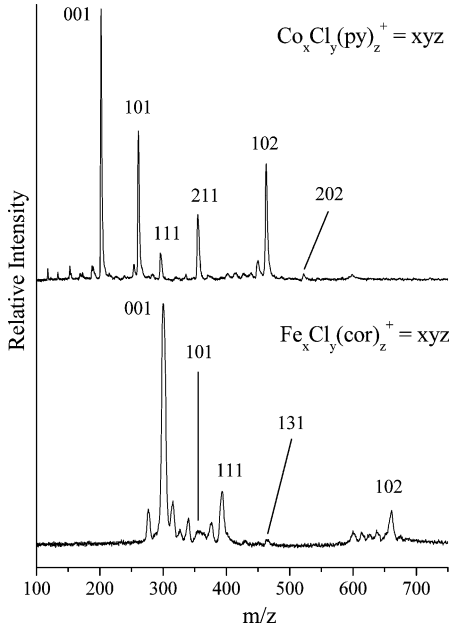

Figure 3. Mass spectra resulting from covaporization of $FeCl_2 \cdot 4H_2O$ or $CoCl_2 \cdot 6H_2O$ with coronene.

atomic cations were produced. In contrast to this result, $Fe^+(cor)_{1,2}$ and $Co^+(cor)_{1,2}$ complexes were produced in large abundance in our molecular beam experiments.[20,24] Likewise, similar experiments combining iron or cobalt powders with pyrene also produced no complexes.

The main difference between these studies and the molecular beam work is that a pulsed nozzle expansion gas is present in the molecular beam experiments. This collision gas can stabilize more weakly bound complexes. It is therefore interesting to consider whether the iron and cobalt complexes are not seen here because they are too weakly bound to survive under the rather hot growth conditions. Bond energies for transition metal cation complexes with PAH species are not generally available. However, in our previous experiments using competitive ligand binding, we estimated that the bond energy for Fe^+(cor) was greater than 48 kcal/mol.[24] To compare the binding energy of iron to those of other transition metal ions, we use the theoretical results of Klippenstein.[47] Figure 2 compares the complex binding tendencies to the binding energies calculated for M^+(cor) monoligand complexes. The calculated binding energies follow a trend not unlike those seen for other metal ion−ligand complexes, with a minimum in bond energy for the Mn^+ complex.[47] However, we find significant amounts of Mn^+(cor) in our experiment. For the problematic metals, iron has a lower binding energy than some other metals, but its binding energy to coronene is still predicted to be substantial, consistent with our previous experiment. On the other hand, cobalt ion has one of the highest predicted binding energies to coronene. Therefore, it does not seem that binding energy trends can explain the poor yields for iron and cobalt complexes. Additionally, even for the other metals that form complexes, the tendency to bind to coronene does not track with the relative bond energies that are calculated. Apparently, the kinetics and dynamics in the plasma growth process are also quite important in the yield of complexes by this method.

Transition Metal Salts + PAH. To further investigate the clustering behavior of iron and cobalt, experiments were performed with vaporization of *metal salts* instead of pure metal powders in mixtures with the PAHs. Figure 3 shows a representative mass spectrum for the covaporization of $FeCl_2 \cdot 4H_2O$ with coronene (lower trace) and a similar spectrum resulting from the covaporization of $CoCl_2 \cdot 6H_2O$ with pyrene (upper trace). As indicated, both metal salt experiments produced PAH mono- and diligand complexes efficiently. In addition to the complexes with the bare metal ions, metal chloride−PAH complexes are also produced for both systems. Higher laser power is required for these experiments, which produces carbon fragment ions above and below the mass of coronene and coronene dimer (near 600 amu). These fragments are also seen without metal whenever high laser power is employed. There is thus a significant difference in the tendency to make the desired metal−PAH complexes depending on the source of the metal. Because the overall concentrations of metal and PAH are comparable in the pure metal versus metal salt experiments, there must be some difference in the reactivity of the metal species produced in these different experiments. To investigate this further, we must consider the mechanism of growth of these complexes under our conditions.

The laser vaporization/ablation process is well-known to produce both neutral and ionized species of both metal and organics. However, there is no post-ionization in our experiment, and we measure only the ions that are produced directly. The complexes can result from the combination of metal cations with neutral PAH species, or vice versa. The electrostatic interactions are much favored for the former case. It is conceivable that complexes could form initially as neutrals and then be ionized by an electron collision in the plasma. However, electron mobility is much greater than atomic or molecular values, and therefore the density of electrons in the growth region with enough energy to ionize drops very quickly because of the acceleration fields present. Likewise, photoionization of neutral complexes is also unlikely because of the low photon energy at 532 nm and because of the laser pulse duration (5 ns), which is short compared to the movement of atoms and molecules. In our previous molecular beam experiments, ionization of neutral PAH complexes produced much lower signal levels than direct sampling of cations.[20−24] Therefore, the most likely mechanism for complex growth here is the combination of metal cations with neutral PAH species. We should therefore focus on the possible differences between cobalt and iron metal ions produced directly by metal vaporization as opposed to those produced by vaporization of metal salts.

The most obvious difference between metal ions produced from pure metal or metal salts is the oxidation state in the precursor material. If metal cations from salts are produced in higher charge states, then it would not be surprising that these ions would have a stronger attraction for PAH surfaces and therefore be more reactive. However, there is no evidence in any of these mass spectra for doubly charged metal ions. It is noticeable that the metal salt samples provide higher yields of singly charged metal, but the yield of metal ion in the neutral powder experiments was large enough that we could have seen complexes.

The next possible issue is the electronic state of the metal cations produced. It is well-known in transition metal ion−molecule chemistry that reactivity can depend dramatically on the electronic state of the cations.[58−61] In particular, Fe^+ and Co^+ produced by various ionization methods are known to exist in a distribution of ground and excited states, and some of the excited states are metastable, so they survive for long periods. Fe^+ has the d^6s^1 (^6D) ground state, with relatively low-lying ^4F and ^4D excited states, while Co^+ has a d^8 (^3F) ground state and low-lying ^5F and ^3F excited states. In both cases, state-specific studies show that the excited states are much more reactive than

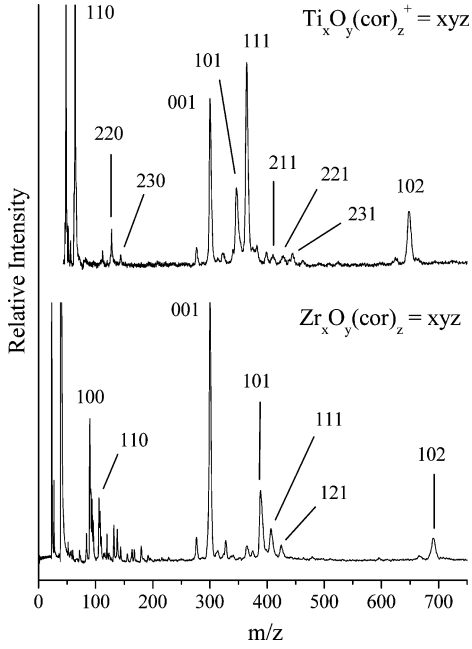

Figure 4. Mass spectra resulting from covaporization of titanium oxide with coronene and of zirconium carbide with coronene.

the ground states.[58−61] A simple explanation for our experiment, therefore, is that metal powder vaporization produces larger quantities of ground state metal ions, while metal salt vaporization produces higher yields of the more reactive excited states. It is not clear why these trends would occur, but it might be possible to test this hypothesis with emission experiments on these plasmas. In light of this result, it is also apparent that the distribution of metal ion electronic states generated in the laser vaporization process and the relative reactivity of these states probably affect all of the metal−PAH complex growth processes. This helps to explain why the tendencies to form complexes do not follow the same trend as complex binding energies.

Another interesting observation is that metal chloride−PAH complexes are formed in the metal salt experiments. Figure 3 shows clearly the presence of $FeCl^+$(cor), $CoCl^+$(py), and Co_2Cl^+(cor) monoligand complexes. There are also large signals for $M^+(PAH)_2$ sandwiches, and even some small signals for $M_2^+(cor)_2$ sandwiches. However, no $MCl^+(PAH)_2$ sandwich ions are detected. This behavior is apparently similar to the situation discussed above, where no $Al^+(PAH)_2$ sandwiches are observed, and a similar explanation makes sense here, too. The first PAH molecule would most likely bind to the positive end of the metal chloride ion, i.e., on the metal. This places the negative chlorine on the side of the MCl^+ species opposite the PAH. If a sandwich species is to form, the second PAH must approach the metal center from this side, and it encounters the strong negative region of the chlorine. The negatively charged chlorine would interact repulsively with the π cloud of the PAH, in much the same way suggested for the negatively charged region of polarized Al^+ ions. The chloride species effectively limits sandwich growth by providing an unfavorable bonding interaction to the second ligand.

Transition Metal Oxides and Carbides + PAH. If the mechanism discussed for inhibition of sandwich growth is valid, then other metal compounds that exhibit ionic bonding should behave in the same way. We therefore decided to examine the clustering behavior of metal oxides or carbides with PAH systems. The early transition metals, titanium, vanadium, and zirconium, produced metal oxide−PAH complexes efficiently in these experiments. Figure 4 shows mass spectra obtained using titanium oxide or zirconium carbide powders in mixtures with coronene. In the upper frame, titanium and various titanium oxide ions are prevalent at low masses. Both titanium monoligand complexes and sandwiches are observed. The most abundant complex produced is the titanium oxide monoligand complex, TiO^+(cor). Other oxide complexes are also seen corresponding to the stoichiometries $Ti_2O_x^+$(cor), with $x = 1-3$. Like the chlorides, however, there are no oxide sandwiches. The data in the lower frame were acquired by covaporizing zirconium carbide and coronene. Surprisingly, there is no indication for any zirconium carbide cluster ion formation. Instead, the ions occurring at low masses include zirconium and zirconium oxide. Apparently, the oxygen comes from gas adsorbed on the surface of the powder samples, which were handled in air. In contrast to the titanium oxide system, the most abundant monoligand complex formed here is the bare metal Zr^+(cor) complex. Other zirconium oxide complexes are formed with the stoichiometry ZrO_x(cor), with $x = 1, 2$. The last prominent mass appearing in the spectrum corresponds to the $Zr^+(cor)_2$ sandwich. As seen for the chloride systems above, there is no evidence here for oxide sandwiches. Similar behavior is found (data not shown) for iron and vanadium oxide clustering with coronene.

Therefore, the clustering behavior of oxide species with these PAH systems follows the same pattern that we saw with aluminum and the metal chlorides. The negative end of the metal oxide apparently behaves in the same way as the chlorides or the polarized valence electron cloud of aluminum, inhibiting the addition of a second PAH molecule. Another related observation is that these trends apply not only for MO^+ diatomics, but also for larger oxides. Titanium and iron produced small amounts of multimetal oxide complexes such as Fe_2O^+(cor) and $Ti_2O_x^+$(cor), for $x = 1-3$. Again, no multimetal oxide sandwiches are observed in either experiment. With these multiple metal oxides, it is natural to wonder if both metals are bound to the same side of coronene, as opposed to two additions of metal and/or oxide on opposite sides of the ring system. Likewise, if binding occurs on the same side of the PAH, are the metals connected or bound separately at different ring sites? However, the same multimetal oxide stoichiometries are observed in the mass spectrum without coronene. Therefore, it is likely that they exist first in the gas phase and then are bound to the PAH as a single unit. This also makes sense in light of the strong metal oxide bonding. Titanium and iron oxide bond energies are 159.8 and 78.4 kcal/mol, respectively,[62] which is much greater than the calculated titanium and iron binding energies to coronene (52.1 and 56.0 kcal/mol respectively).[19,47] The simplest assumption then is that the metal oxide attaches as a single unit to the PAH molecule.

Lanthanides and Actinides + PAH. To investigate other interesting metals and their oxides, we examined neodymium and uranium as representatives of the lanthanide and actinide metals. Figure 5 shows the mass spectra for experiments on the covaporization of neodymium oxide and pyrene (upper trace) and on the covaporization of uranyl acetate and pyrene. Large amounts of atomic metal and oxide ions are produced in both spectra. Pure metal monoligand complexes and sandwich species are observed for both neodymium and uranium. Monoligand metal oxide−PAH complexes, MO^+(PAH), are prevalent in these spectra, like those observed for titanium, vanadium, and zirconium. However, one major difference between the rare earths and transition metal species becomes apparent. Significant amounts of metal oxide−PAH sandwich complexes,

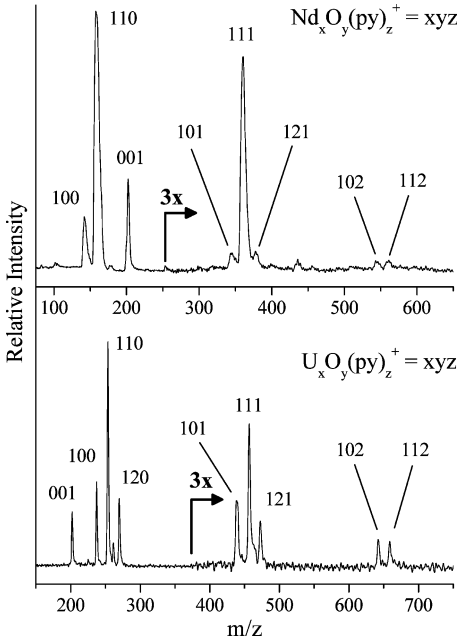

Figure 5. Mass spectra resulting from covaporization of neodymium oxide with pyrene and uranyl acetate (UAc) with pyrene.

$MO^+(PAH)_2$, are observed for both neodymium and uranium. It is therefore interesting to consider why these oxide sandwiches form, while those of the transition metals do not. A possible explanation for this behavior lies in the different ionic radii of the metals, which would affect the ability of oxygen to screen the second ligand from the charge of the metal. The ionic radii of first- and second-row transition metals in the +1 oxidation state, which is probably appropriate to consider for these MO^+ species, all fall in the range of 0.8−1.0 Å.[63] If the appropriate picture is more like M^{2+},O^-, then the positively charged volume would have an even smaller size. The size of the transition metals is apparently not large enough to offset the region of negative charge coming from the oxygen atoms, and consequently, the second PAH ligands do not bind effectively to these oxides. Information on the ionic radii of the +1 or +2 oxidation states of neodymium or uranium is not generally available because these are not the common oxidation states for these metals. However, the +3 oxidation states for these metals have radii of 1.12 and 1.16 Å, respectively.[63] The sizes of the metal atoms in the partially oxidized NdO^+ and UO^+ ions are almost certainly larger than this. Therefore, these heavier metal ions would occupy a larger volume of positive charge, and it is conceivable that this metal atom size would outweigh the oxygen atom charge screening from the standpoint of ligand interactions. This size effect could explain why the binding of second ligands in these sandwich species occurs more readily in these systems. It is also conceivable that the different strengths of attractive forces in these metal ions come into play. Unlike the transition metals, the heavier systems could have more M^{3+},O^{2-} character in their diatomic oxides. This higher charge density would result in a greater long-range attraction for a second PAH ligand, perhaps also contributing to the improved sandwich formation in these systems.

Organometallics + PAH. Having seen that metal salts and oxides produce PAH complexes, we decided to investigate the covaporization of PAH powders with other organometallic complexes. These species are of interest because they could form mixed-ligand sandwich complexes. A limited number of mixed-ligand complexes of iron have been produced in conventional synthetic chemistry.[64−66] However, these synthesis methods are problematic because of the poor solubility of PAH systems. It is therefore interesting to see if covaporization methods would produce similar mixed-ligand complexes. Initial experiments employing ferrocene mixtures with coronene or pyrene were unsuccessful, presumably because of the high stability of ferrocene.[67] A strong ferrocene parent ion was observed, but no reaction products. Presumably, dissociation in the plasma is required for reaction, and ferrocene does not dissociate efficiently. We next examined iron cyclopentadienyl benzene, Fe(cp)(bz), a molecule similar to ferrocene but with one of the cyclopentadiene ligands replaced by benzene. While ferrocene is an 18-electron species as a neutral complex, Fe(cp)(bz) is an 18-electron species as a cation. Even so, the latter complex has a lower stability than ferrocene,[68] and it dissociates easily under our conditions. Figure 6 shows a mass spectrum of the covaporization of a mixed powder sample of Fe(cp)(bz) and coronene. The primary fragments of Fe(cp)(bz) include Fe^+ and $Fe(cp)^+$ under all laser power conditions. Coronene and ferrocene appear as the largest ions in abundance; decomposition of Fe(cp)(bz) is the most likely source of ferrocene. The main complexes produced by the decomposition/reaction process in the plasma include $Fe^+(cp)(cor)$ and $Fe^+(cor)_2$, while a minor amount of $Fe^+(bz)(cor)$ is also detected.

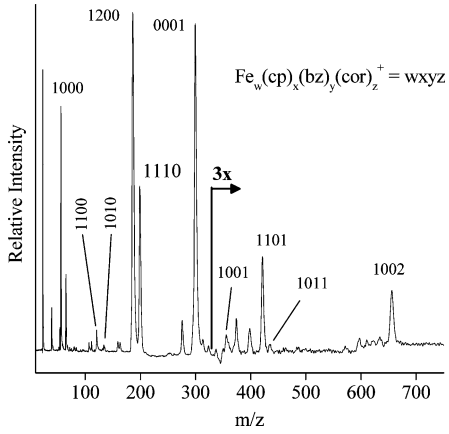

Figure 6. Mass spectra resulting from covaporization of iron cyclopentadienyl benzene and coronene.

This approach therefore provides yet another method of producing metal−PAH complexes. The relative abundance of the different mixed-ligand and monoligand complexes can be rationalized simply on the basis of metal−ligand bond energies. The $Fe^+(cp)$ bond energy is far greater than that of $Fe^+(bz)$,[67,68] so benzene is more likely to be eliminated first in the plasma dissociation of Fe(cp)(bz). Consistent with this, the reaction product $Fe^+(cp)(cor)$ is also produced in much larger abundance than $Fe^+(bz)(cor)$. Since the ratio of $Fe^+(cp)$ to $Fe^+(bz)$ is similar to the ratio of $Fe^+(cp)(cor)$ to $Fe^+(bz)(cor)$, it can be assumed that the primary mechanism of coronene complex production involves the reaction of the fragments of Fe(cp)(bz) with coronene vapor created in the vaporization process. The amount of coronene vapor present upon vaporization should be much greater than the amount of benzene and cyclopentadiene produced by the fragmentation of Fe(cp)(bz). Therefore, the principle reaction of the iron cation produced by continued fragmentation must be with coronene. This same reasoning explains why no $Fe^+(bz)_2$ is present in the spectrum. Very little $Fe^+(bz)$ is produced in the dissociation process, and only a low concentration of benzene is available for reaction. The large amount of coronene vapor present in the environment makes this pathway unlikely. Additionally, the iron−benzene bond is the weakest of the metal−ligand interactions investigated here

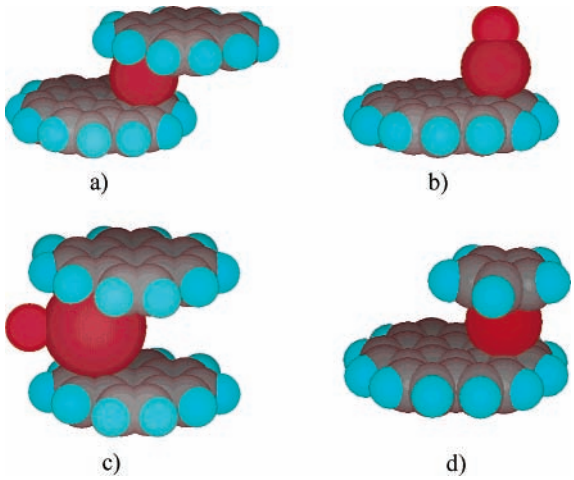

Figure 7. Schematic structures expected for various complexes studied here. In (a), the mixed-ligand complex M^+(cor)(py) is shown. The binding to outer rings on both PAH species leads to an expected staggered sandwich structure. In (b), the complex MX^+(cor) is shown, for X = O, Cl, etc., with M binding downward to an outer ring site. (c) shows the complex $NdO^+(cor)_2$, with the metal oxide approximately to scale, and outer ring binding on the coronene. (d) shows the Fe^+-(cp)(cor) mixed sandwich, also with outer ring binding on the coronene.

at 37.8−44.7 kcal/mol.[69,70] Klippenstein has previously calculated the Fe^+(cor) bond energy to be approximately 56 kcal/mol.[47] Our previous photodissociation experiments also found that iron binding to benzene was weaker than iron binding to coronene.[17]

In contrast to the ferrocene result, the reaction of dibenzene chromium, $Cr(bz)_2$, with coronene proved to be more interesting. A laser vaporization experiment performed in the absence of PAH showed that $Cr(bz)_2$ fragments in the laser plasma by losing both benzenes, producing a strong Cr^+ ion in the mass spectrum. The bond dissociation energy in this sandwich system (47.0−55.3 kcal/mol) is much lower than that for ferrocene (91 kcal/mol),[47,67] allowing more efficient dissociation of the complex in the plasma. When $Cr(bz)_2$ was combined with coronene (data not shown), no Cr^+(bz) or Cr^+(bz)(cor) ions were detected, but a substantial amount of $Cr^+(cor)_2$ was formed. The calculated Cr^+(cor) bond energy (46.2 kcal/mol)[47] is larger than that of Cr^+(bz) (36.4 kcal/mol), which can explain the strong tendency for chromium ions to bind to coronene instead of benzene in this experiment.

Structures and Growth Trends. Having discussed the variety of metal−PAH complexes that can be formed, it is natural to consider the structures of these systems. We have discussed some of these previously.[20−24] In intercalated graphite[71] and in other organometallic complexes, metals bind in η^6 ring sites, and therefore we assume that the same will be true here. However, theoretically other binding sites, such as metal localized over a double bond, may also be possible.[48] In coronene, previous experiments on synthetic analogues show that metal binds to the outer ring sites.[64−66] NMR spectroscopy shows that the highest electron density is found in alternate outer ring sites.[72] Likewise, the rings in pyrene are also not equivalent, with the highest electron density lying in the outer rings.[73] Complexes of various types would therefore likely have metal, metal halide, or metal oxide species binding to these outer ring sites. Sandwich complexes of the form $M^+(cor)_2$ or $M^+(py)_2$ would therefore likely have staggered structures rather than parallel because of the π repulsion of ring systems away from the metal.[24] Figure 7 shows schematic structures that would result from these considerations. Also shown is the sandwich structure of $NdO^+(cor)_2$, with the atoms drawn approximately to scale. This structure shows one way in which the sandwich can form for this species, and how the size of Nd minimizes the effect of the repulsive interaction of the oxygen.

Taken together, these various experiments identify a number of general tendencies for the formation of metal−PAH complexes using laser vaporization methods. Complexes can be produced from the vaporization of mixed powders containing pure metal and PAH species, from the vaporization of mixed powders containing PAH and metal salts or oxides, and from mixed powders containing PAH and organometallic complexes. In all cases, metal cation complexes form rather efficiently in general. However, an anomaly in complex growth occurs for iron and cobalt, where complexes do not form from pure metal powders, but do form easily from metal salts, oxides, or organometallics. The formation of complexes in such a laser vaporization process is not simple, and it is not easy to probe the mechanism of this process. Additionally, we only detect the positive ions that form, and are not able to observe neutrals in these experiments. Negative ions of these metal−PAH systems have been produced previously in our molecular beam experiments,[74] but we did not investigate these species in this work. The most likely mechanism consistent with our data is that metal ions are produced in the gas phase following the initial laser impact, and then these cations react with neutral PAH species, producing the complexes. The iron and cobalt data can be explained if laser vaporization of pure metal produces mostly unreactive ground state cations, while other vaporization processes produce more reactive excited states.

In addition to the electronic state of the metal cations produced, complex formation also apparently depends on other factors such as the metal−organic bond energies. Consistent with this idea, we are able to make mixed sandwiches of iron with cyclopentadiene, but not with benzene. However, energetics alone are not enough to understand the growth processes. For example, calculations by Klippenstein indicate that the Fe^+(cor) bond energy is stronger than those predicted for the early transition metals.[47] Surprisingly, early transition metals in our experiments produced complexes more efficiently than iron. Ionization potentials of the metals play an indirect role in the production of these complexes. The early first-row transition metals (Sc to Cr) have ionization potentials on average 1 eV lower than all of the later transition metals. This likely explains the more efficient production of atomic metal cation for these metals, which in turn results in greater amounts of complexes. Similarly, atomic metal cations were also produced more efficiently in experiments with metal salts, oxides, and organometallics than they were from pure metals, presumably because of their oxidation states in these compounds. Consequently, complex formation was also efficient in these experiments, even for systems other than iron and cobalt that had no apparent electronic state issues.

No multimetal−PAH complexes were observed in these experiments except for the Fe_2O^+, Co_2Cl^+, and $Ti_2O_x^+$ species. This is in contrast to molecular beam experiments performed by our group, where many multimetal complexes are seen.[20−24] The simplest reason for this difference is the absence of a collision gas in the present experiments. In these experiments, temperatures generated in the cluster source are much higher than in pulsed nozzle experiments, and the vaporized species also experience fewer collisions. Thus, only small clusters with relatively high bond energies will survive. The molecular species best able to survive these extreme conditions are the strongly

bound oxides, and therefore the complexes with these species are understandable.

It is interesting to speculate on the implications of this work for interstellar condensation processes that might lead to the formation of metal−PAH species. Iron, magnesium, and aluminum are some of the most abundant metals in these environments.[75] Apparently, aluminum and magnesium ions may condense on PAH surfaces to form monoligand complexes, but sandwich species are unlikely to form with these metals. Likewise, iron cations are apparently unreactive unless they are produced in excited states, and therefore condensation with PAHs may not be efficient in the interstellar environment. Because metal oxides are so strongly bound, they are one of the first molecular species to form in stellar outgrowths,[75] and the condensation of these species on PAH surfaces appears to be relatively efficient. However, sandwich formation is again not likely to be efficient.

In the experiments shown here, we have employed pyrene and coronene because of their convenient low vapor pressures. We found similar efficiencies for complex formation with both of these systems. In our molecular beam experiments, we also found similar efficiencies for several other PAH systems. It is therefore reasonable to expect that a variety of metal ion−PAH complexes could be produced with the methods described here. We were therefore surprised to find that these methods were unsuccessful for the production of metal−C_{60} complexes. In selected experiments combining C_{60} with Cr powder, iron chloride, titanium oxide, or zirconium carbide, we were not able to observe any metal complexes. On the other hand, in our previous molecular beam work, many metal−C_{60} complexes were produced,[16,17] also including mixed sandwiches with PAHs.[24] However, we did show that metal−C_{60} complexes were not as strongly bound as corresponding metal cation−coronene complexes or even M^+−benzene complexes.[24] Apparently, this weaker binding tendency limits the efficiency of metal−C_{60} complexes in these experiments without a collision gas present. On the other hand, recent experiments in our group have demonstrated the formation of metal and nonmetal complexes with the bowl-shaped corannulene ($C_{20}H_{10}$) molecule.[76] The methods described here therefore have some limitations, but they are applicable to a variety of metal−molecular systems.

Conclusions

We describe the production of a variety of ion−molecule complexes between metal cations and coronene or pyrene. These complexes are produced using laser vaporization of mixed powder samples containing the PAH of interest together with pure metal, metal halides, metal oxides, metal carbides, or organometallic complexes. The tendency of metals to form complexes varies, but not in a way that corresponds directly to bonding energetics. However, it is clear that bonding energetics do play a role in these systems, especially in systems where the same metal reacts with different ligands. Additionally, cobalt and iron systems vary dramatically in their tendencies to form complexes depending on the source of the metal. Apparently some vaporization systems produce metal cations in reactive excited electronic states, and these systems form complexes more efficiently. It is clear from these studies that metal cation chemistry in these laser plasmas is complex, as noted previously by many other research groups.

We do not observe efficient production of multiple metal atom complexes on individual PAH molecules or multimetal sandwiches. Likewise, we do not see efficient production of systems with more than two PAH molecules. These more highly aggregated systems can be formed in molecular beam experiments, where expansion gases are present and provide a means for collision stabilization. Likewise, we are also not able to form metal−C_{60} complexes by these methods, presumably because the binding energies for these systems are lower than they are for the PAH complexes. However, we do form a wide variety of metal and metal compound complexes as well as mixed-ligand species with two PAH species or with one PAH and either benzene or cyclopentadiene. This method of complex formation is therefore versatile, and can be implemented in many different mass spectrometers to enable studies of reaction kinetics and ligand displacement processes in these systems.

Acknowledgment. This work is supported by the Air Force Office of Scientific Research (Grant F49620-00-1-0118) and the Petroleum Research Fund of the American Chemical Society (Grant 36946-AC6).

References and Notes

(1) Hoshino, K.; Kurikawa, T.; Takeda, H.; Nakajima, A.; Kaya, K. *J. Phys. Chem.* **1995**, *99*, 3053.
(2) Judai, K.; Hirano, M.; Kawamata, H.; Yabushita, S.; Nakajima, A.; Kaya, K. *Chem. Phys. Lett.* **1997**, *270*, 23.
(3) Yasuike, T.; Nakajima, A.; Yabushito, S.; Kaya, K. *J. Phys. Chem. A* **1997**, *101*, 5360.
(4) Nagao, S.; Kato, A.; Nakajima, A.; Kaya, K. *J. Am. Chem. Soc.* **2000**, *122*, 4221.
(5) Nagao, S.; Kurikawa, T.; Miyajima, K.; Nakajima, A.; Kaya, K. *J. Phys. Chem. A* **1998**, *102*, 4495.
(6) Nakajima, A.; Kaya, K. *J. Phys. Chem. A* **2000**, *104*, 176.
(7) Kurikawa, T.; Negishi, Y.; Hayakawa, F.; Nagao, S.; Miyajima, K.; Nakajima, A.; Kaya, K. *Eur. Phys. J. D* **1999**, *9*, 283.
(8) Martin, T. P.; Malinowski, N.; Zimmermann, U.; Naher, U.; Schaber, H. J. *J. Chem. Phys.* **1993**, *99*, 4210.
(9) Zimmermann, U.; Malinowski, N.; Naher, U.; Frank, S.; Martin, T. P. *Phys. Rev. Lett.* **1994**, *72*, 3542.
(10) Tast, F.; Malinowski, N.; Frank, S.; Heinebrodt, M.; Billas, I. M. L.; Martin, T. P. *Phys. Rev. Lett.* **1996**, *77*, 3529.
(11) Tast, F.; Malinowski, N.; Heinebrodt, M.; Billas, I. M. L.; Martin, T. P. *J. Chem. Phys.* **1997**, *106*, 9372.
(12) Kurikawa, T.; Nagao, S.; Miyajima, K.; Nakajima, A.; Kaya, K. *J. Phys. Chem. A* **1998**, *102*, 1743.
(13) Nagao, S.; Negishi, Y.; Kato, A.; Nakamura, A.; Nakajima, A.; Kaya, K. *J. Phys. Chem. A* **1999**, *103*, 8909.
(14) Palpant, B.; Otake, A.; Hayakawa, F.; Negishi, Y.; Lee, G. H.; Nakajima, A.; Kaya, K. *Phys. Rev. B* **1999**, *60*, 4509.
(15) Palpant, B.; Negishi, Y.; Senekata, M.; Miyajima, K.; Nagao, S.; Judai, K.; Rayner, D. M.; Simard, B.; Hackett, P. A.; Nakajima, A.; Kaya, K. *J. Chem. Phys.* **2001**, *114*, 8459.
(16) Reddic, J. E.; Robinson, J. C.; Duncan, M. A. *Chem. Phys. Lett.* **1997**, *279*, 203.
(17) Grieves, G. A.; Buchanan, J. W.; Reddic, J. E.; Duncan, M. A. *Int. J. Mass Spectrom.* **2001**, *204*, 223.
(18) Dunbar, R. C.; Uechi, G. T.; Asamoto, B. *J. Am. Chem. Soc.* **1994**, *116*, 2466.
(19) Ho, Y. P.; Yang, Y. C.; Klippenstein, S. J.; Dunbar, R. C. *J. Phys. Chem.* **1997**, *101*, 3338.
(20) Buchanan, J. W.; Reddic, J. E.; Grieves, G. A.; Duncan, M. A. *J. Phys. Chem. A* **1998**, *102*, 6390.
(21) Buchanan, J. W.; Grieves, G. A.; Flynn, N. D.; Duncan, M. A. *Int. J. Mass Spectrom.* **1999**, *185−187*, 617.
(22) Foster, N. R.; Grieves, G. A.; Buchanan, J. W.; Flynn, N. D.; Duncan, M. A. *J. Phys. Chem. A* **2000**, *104*, 11055.
(23) Foster, N. R.; Buchanan, J. W.; Flynn, N. D.; Duncan, M. A. *J. Chem. Phys.* **2001**, *341*, 476.
(24) Buchanan, J. W.; Grieves, G. A.; Reddic, J. E.; Duncan, M. A. *Int. J. Mass Spectrom.* **1999**, *182/183*, 323.
(25) Klotz, A.; Marty, P.; Boissel, P.; de Caro, D.; Serra, G.; Mascetti, J.; de Parseval, P.; Derouault, J.; Daudey, J.-P.; Chaudret, B. *Planet. Space. Sci.* **1996**, *44*, 957.
(26) Doina, C.; Bohme, D. K. *Int. J. Mass Spectrom.* **2003**, *223−224*, 411.
(27) Cassam-Chenai, P. *Planet. Space Sci.* **2002**, *50*, 871.
(28) Harvey, R. G. *Polyaromatic Hydrocarbons*; Wiley-VCH: New York, 1996.
(29) Birks, J. B. *Photophysics of Aromatic Molecules*; John Wiley: London, 1970.

(30) Klessinger, M.; Michl, J. *Excited States and Photochemistry of Organic Molecules*; VCH Publishers: New York, 1995.
(31) *Spectral Atlas of Polyaromatic Hydrocarbons*; Karcher, W., Fordham, R. J., Dubois, J. J., Glaude, P. G. J. M., Lighthart, J. A. M., Eds.; D. Reidel Publishers: Dordrecht, 1985.
(32) Bohme, D. K. *Chem. Rev.* **1992**, *92*, 1487.
(33) *The Diffuse Interstellar Bands*; Tielens, A. G. G. M., Snow, T. P., Eds.; Kluwer Academic Publishers: Dordrecht, 1995.
(34) Salama, F.; Bakes, E. L. O.; Allamandola, L. J.; Tielens, A. G. G. M. *Astrophys. J.* **1996**, *458*, 621.
(35) Henning, T.; Salama, F. *Science* **1998**, *282*, 2204.
(36) Brechignac, P.; Pino, T.; Boudin, N. *Spectrochim. Acta A* **2001**, *57*, 745.
(37) Allamandola, L. J.; Tielens, A. G. G. M.; Barker, J. R. *Astrophys. J. Suppl.* **1989**, *71*, 733.
(38) Leger, A.; d'Hendecourt, L.; Defourneau, D. *Astron. Astrophys.* **1989**, *216*, 148.
(39) Dresselhaus, M. S.; Dresselhaus, G. *Adv. Phys.* **2002**, *51*, 1.
(40) *Intercalation Chemistry*; Whittingham, M. S., Jacobson, A., Eds.; Academic Press: New York, 1982.
(41) *Graphite Intercalation Compounds and Applications*; Enoki, T., Suzuki, M., Endo, M., Eds.; Oxford University Press: New York, 2003.
(42) *Science of Fullerenes and Carbon Nanotubes*; Dresselhaus, M. S., Dresselhaus, G., Eklund, P. C., Eds.; Academic Press: San Diego, 1996.
(43) Chaudret, B.; Le Beuze, A.; Rabaa, H.; Saillard, J. Y.; Serra, G. *New J. Chem.* **1991**, *15*, 791.
(44) Serra, G.; Chaudret, B.; Saillard, Y.; Le Beuze, A.; Rabaa, H.; Ristorcelli, I.; Klotz, A. *Astron. Astrophys.* **1992**, *260*, 489.
(45) Boissel, P. *Astron. Astrophys.* **1984**, *285*, L33.
(46) Dunbar, R. C. *J. Phys. Chem. A* **2002**, *106*, 9809.
(47) Klippenstein, S. J.; Yang, C.-N. *Int. J. Mass Spectrom.* **2001**, *201*, 253.
(48) Senapati, L.; Nayak, S. K.; Rao, B. K.; Jena, P. *J. Chem. Phys.* **2003**, *118*, 8671.
(49) Cornett, D. S.; Amster, I. J.; Duncan, M. A.; Rao, A. M.; Eklund, P. C. *J. Phys. Chem.* **1993**, *97*, 5036.
(50) Wiley, W. C.; McLaren, I. H. *Rev. Sci. Instrum.* **1955**, *26*, 1150.
(51) Sodupe, M.; Bauschlicher, C. W. *J. Chem. Phys. Lett.* **1991**, *181*, 321.
(52) Bauschlicher, C. W.; Partridge, H. *J. Phys. Chem.* **1991**, *95*, 9694.
(53) Sodupe, M.; Bauschlicher, C. W.; Partridge, H. *Chem. Phys. Lett.* **1992**, *192*, 185.
(54) Bauschlicher, C. W.; Sodupe, M.; Partridge, H. *J. Chem. Phys.* **1992**, *96*, 4453.
(55) Gregoire, G.; Brinkmann, N. R.; Schaefer, H. F.; Duncan, M. A. *J. Phys. Chem. A* **2003**, *107*, 218.
(56) Walters, R. S.; Brinkmann, N. R.; Schaefer, H. F.; Duncan, M. A. *J. Phys. Chem. A* **2003**, *107*, 7396.
(57) (a) Inokuchi, Y.; Ohshimo, K.; Misaizu, F.; Nishi, N. *J. Phys. Chem. A* **2004**, *108*, 5034. (b) Inokuchi, Y.; Ohshimo, K.; Misaizu, F.; Nishi, N. *Chem. Phys. Lett.* **2004**, *390*, 140.
(58) (a) Van Koppen, P. A. M.; Kemper, P. R.; Bowers, M. T. *J. Am. Chem. Soc.* **1992**, *114*, 10941. (b) Van Koppen, P. A. M.; Kemper, P. R.; Bowers, M. T. *J. Am. Chem. Soc.* **1992**, *114*, 1083.
(59) Weisshaar, J. C. *Acc. Chem. Res.* **1993**, *26*, 213.
(60) Armentrout, P. B. *Annu. Rev. Phys. Chem.* **1990**, *41*, 313.
(61) Fisher, E. R.; Elkind, J. L.; Clemmer, D. E.; Georgiadis, R.; Loh, S. K.; Aristov, N.; Sunderlin, L. S.; Armentrout, P. B. *J. Chem. Phys.* **1990**, *93*, 2676.
(62) Fisher, E. R.; Elkind, J. L.; Clemmer, D. E.; Georgiadis, R.; Loh, S. K.; Aristov, N.; Sunderlin, L. S.; Armentrout, P. B. *J. Chem. Phys.* **1990**, *93*, 2676.
(63) Huheey, J. E.; Keiter, E. A.; Keiter, R. L. *Inorganic Chemistry: Principles of Structure and Reactivity*, 4th ed.; Harper-Collins: New York, 1993.
(64) Schmitt, G.; Kein, W.; Fleischhauer, J.; Walbergs, U. *J. Organomet. Chem.* **1978**, *152*, 315.
(65) Morrison, W. H.; Ho, E. Y.; Hendrickson, D. N. *Inorg. Chem.* **1975**, *14*, 500.
(66) Astruc, D. *Tetrahedron* **1983**, *39*, 4027.
(67) Lewis, K. E.; Smith, G. P. *J. Am. Chem. Soc.* **1984**, *106*, 4650.
(68) Meyer, F.; Khan, F. A.; Armentrout, P. B. *J. Am. Chem. Soc.* **1995**, *117*, 9740.
(69) Kang, H.; Beauchamp, J. L. *J. Phys. Chem.* **1985**, *89*, 3364.
(70) Loh, S. K.; Fisher, E. R.; Lian, L.; Schultz, R. H.; Armentrout, P. B. *J. Phys. Chem.* **1989**, *93*, 3159.
(71) Müller, U. *Inorganic Structural Chemistry*; John Wiley: Chichester, 1993.
(72) Schmitt, G.; Kein, W.; Fleischhauer, J.; Walbergs, U. *J. Organomet. Chem.* **1978**, *152*, 315.
(73) Steiner, E.; Fowler, P. W.; Jenneskens, L. W.; Havenith, R. W. A. *Eur. J. Org. Chem.* **2002**, 163.
(74) Duncan, M. A.; Knight, A. M.; Negeshi, Y.; Nagoa, S.; Judai, K.; Nakajima, A.; Kaya, K. *J. Phys. Chem. A* **2001**, *105*, 10093.
(75) *The Molecular Astrophysics of Stars and Galaxies*; Hartquist, T. W., Williams, D. A., Eds.; Clarendon Press: Oxford, 1998.
(76) Ayers, T. A.; Westlake, B. C.; Duncan, M. A., to be submitted.